

DØ Note 5194-CONF

**Search for the Higgs boson
in $H \rightarrow WW^* \rightarrow \mu\mu$ decays with 930 pb^{-1} at DØ in Run II**

The DØ Collaboration
URL <http://www-d0.fnal.gov>
(Dated: July 21, 2006)

A search for the Higgs boson in $H \rightarrow WW^* \rightarrow \mu\mu$ decays in $p\bar{p}$ collisions at a center-of-mass energy of $\sqrt{s} = 1.96 \text{ TeV}$ is presented. The data, corresponding to an integrated luminosity of $\sim 930 \text{ pb}^{-1}$, have been collected from April 2002 to February 2006 with the Run II DØ detector. No significant excess above the Standard Model background has been observed.

Preliminary Results for Summer 2006 Conferences

I. INTRODUCTION

In this note a search for Higgs bosons decaying to the WW^* final state in the $D\bar{O}$ experiment at the Tevatron is presented. To achieve a good signal-to-background ratio, the leptonic decay mode $H \rightarrow WW^* \rightarrow \mu\mu\nu\bar{\nu}$ is considered, leading to a final state with two muons and missing transverse momentum. Searches in this decay mode are particularly sensitive to a Higgs Bosons with mass around 160 GeV [1–3]. If combined with searches exploiting the WH and ZH associated production, this decay mode also increases the sensitivity for the Higgs boson searches in the low mass region $M_H \sim 120$ GeV.

Upper limits on the $H \rightarrow WW^* \rightarrow \mu\mu$ cross section with smaller data sets have already been presented in Ref. [4]. In the present analysis the larger $D\bar{O}$ dataset available is included. An analysis of $H \rightarrow WW^* \rightarrow ll'$ ($l, l' = e, \mu$) using 1 fb^{-1} of data can be found in Ref. [5]. The data sample used in this analysis has been collected between April 2002 and February 2006 by the $D\bar{O}$ detector at the Fermilab Tevatron collider at $\sqrt{s} = 1.96$ TeV.

The main components of the $D\bar{O}$ Run II detector [6] important to this analysis are described briefly. The main detector systems include a magnetic spectrometer, a calorimeter and a muon detector.

The central detector consists of the silicon microstrip tracker (SMT) and the central fiber tracker (CFT) within a 2 T solenoidal magnetic field. In the central region the SMT is composed of six alternating axial barrel and radial disk detector components. Five additional disks on either side extend the forward tracking up to pseudo-rapidities of $|\eta_{\text{det}}| \sim 2.5$ for particles originating from the center of the detector. The six barrel segments consist of 4 super-layers of silicon detectors covering a radius from 2.7 to 9.4 cm. The SMT is encased by the CFT with an outer radius of 52 cm. The CFT consists of eight layers of scintillating fiber strips. Each of the layers is composed of 2 doublet layers. Light signals are transferred using fibers to solid-state photon counters (VLPC) that have a quantum efficiency of about 80%.

The calorimeter is a liquid argon sampling calorimeter. It is comprised of a central calorimeter (CC) covering a region up to a pseudo-rapidity of $|\eta_{\text{det}}| \approx 1.1$ and two end calorimeters (EC) extending the coverage to $|\eta_{\text{det}}| \approx 4.2$. The calorimeter is separated into an electromagnetic section (20 radiation lengths), a fine hadronic layer and a coarse hadronic layer.

The muon system consists of one layer inside and two layers outside of an iron toroid magnet with a field strength of 1.8 T inside the iron. Each layer consists of scintillators for fast triggering and drift tubes for position and momentum measurement. Tracking in the muon system for $|\eta| < 1$ relies on 10 cm wide drift tubes [7], while 1 cm mini-drift tubes are used for $1 < |\eta| < 2$ [8].

II. EVENT SELECTION

The $H \rightarrow WW^* \rightarrow \mu\mu$ candidates are selected by triggering on single or di-muon events using a three level trigger system. The first trigger level selects muon candidates formed by hits in two layers of the muon scintillator system. Digital signal processors in the second trigger level form muon track candidate segments defined by hits in the muon drift chambers and scintillators. At the third level, software algorithms running on a computing farm and exploiting the full event information are used to make the final selection of events which are recorded for offline analysis.

In the further offline analysis Muon tracks are reconstructed from hits in the wire chambers and scintillators in the muon system and must match a track in the central tracker. To select isolated muons, the scalar sum of the transverse momentum of all tracks other than that of the muon in a cone of $\mathcal{R} = 0.5$ around the muon track must be less than 4 GeV, where $\mathcal{R} = \sqrt{(\Delta\phi)^2 + (\Delta\eta)^2}$ and ϕ is the azimuthal angle. In addition the energy E_{iso} deposited in a hollow cone with radius $0.1 < \mathcal{R} < 0.4$ around the position of the muon track in the calorimeter must be lower than 4 GeV for the leading muon. For the next-to-leading muon this requirement increases linearly from $E_{\text{iso}} < 1.0$ GeV for 10 GeV muons to $E_{\text{iso}} < 2.5$ GeV for muons with a momentum of 30 GeV or more. This selection is designed to reject background from $W + jet \rightarrow \mu\nu + jet$ events where the second muon comes from a jet. QCD background is selected from data by inverting the isolation criteria to $4 \text{ GeV} < E_{\text{iso}} < 15 \text{ GeV}$. Muon detection is restricted to the coverage of the muon system $|\eta| < 2.0$. Muons from cosmic rays are rejected by requiring a timing criterion on the hits in the scintillator layers as well as applying restrictions on the position of the muon track with respect to the primary vertex.

Two muons are required to be of opposite charge, and must have $p_T > 15$ GeV for the leading muon and $p_T > 10$ GeV for the trailing one. At least one of the muons must have an SMT hit.

A cut on the missing transverse energy in the event $\cancel{E}_T > 20$ GeV is applied to suppress the large Z/γ^* background. Fig. 1 (left) shows the missing transverse energy distribution after preselection.

Events are removed if the \cancel{E}_T could have been produced by a mis-measurement of jet energies. A \cancel{E}_T significance variable is defined by normalizing the \cancel{E}_T to $\sigma(E_T^j \parallel \cancel{E}_T)$, a measure of the jet energy resolution projected onto the

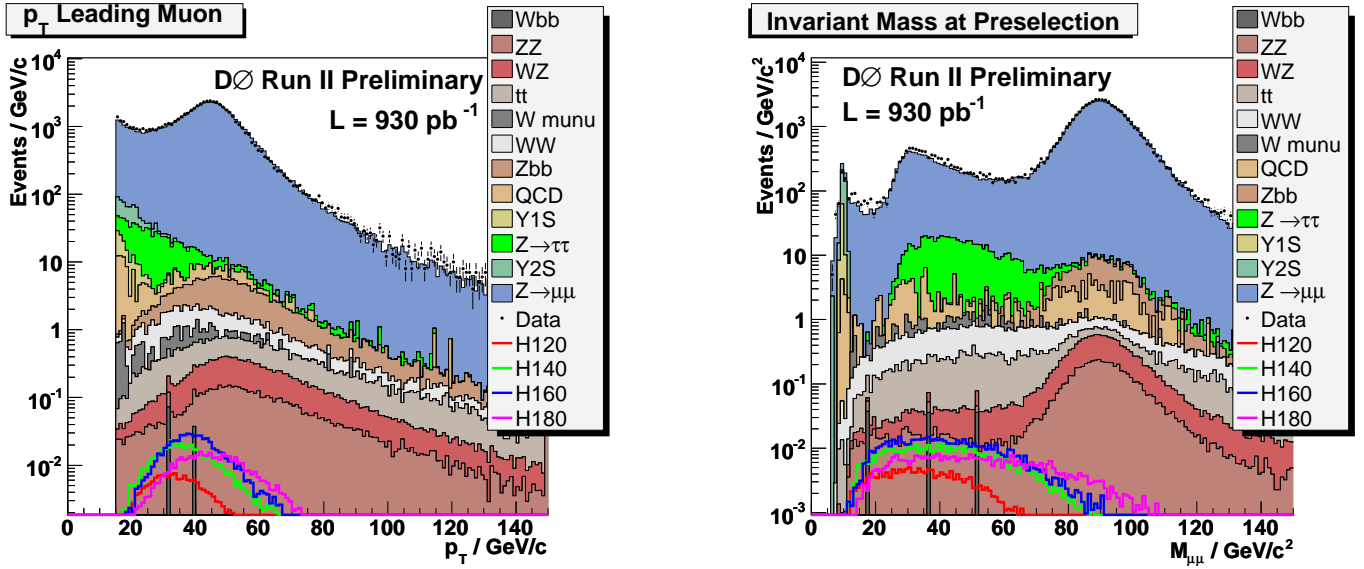


FIG. 1: Distribution of the leading muon momentum and the invariant mass after preselection for data (points) and sum of all backgrounds (filled histograms). The expected signal, multiplied by a factor of 10, for the Standard Model Higgs is also shown.

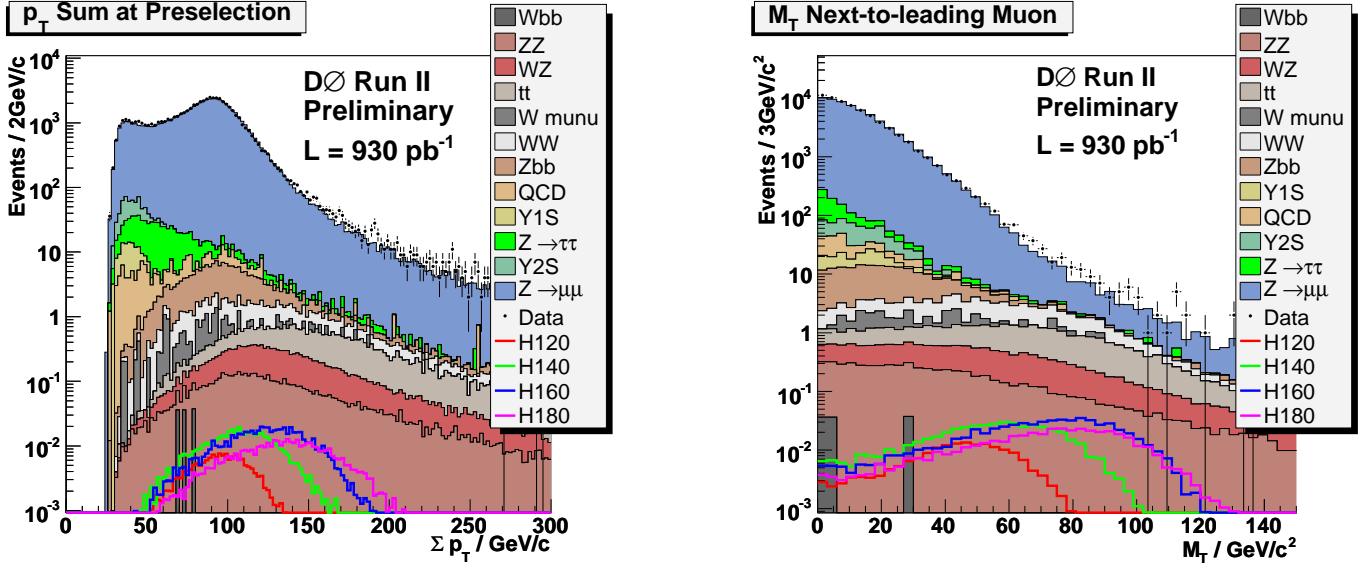


FIG. 2: Distribution of the sum of the lepton transverse momenta and the transverse mass of the next-to-leading muon after preselection. The expected signal, multiplied by a factor of 10, for the Standard Model Higgs is also shown.

\cancel{E}_T direction:

$$\text{Sig}(\cancel{E}_T) = \frac{\cancel{E}_T}{\sqrt{\sum_{\text{jets}} \sigma_{E_T^j}^2 \cancel{E}_T}},$$

where the sum is over all good jets in the event. $\text{Sig}(\cancel{E}_T)$ is required to be greater than 7.

If the \cancel{E}_T in an event comes from a mismeasured lepton the transverse mass of that lepton $M_T(\mu, \cancel{E}_T)$ will be small. A selection of $M_T(\mu, \cancel{E}_T) > 55$ GeV is applied for both muons.

A cut on the invariant dimuon mass $15 \text{ GeV} < M_{\mu\mu} < 80 \text{ GeV}$ removes remaining background from $Z/\gamma^* \rightarrow \mu\mu$ decays. Fig. 1 shows the invariant mass distribution at preselection.

The distribution of the sum of the lepton transverse momenta and the missing transverse energy $p_T(\mu_1) + p_T(\mu_2) + \cancel{E}_T$ after preselection is shown in Fig. 2. Selecting events with a p_T sum between 100 GeV and 160 GeV removes

Selection criterion	Value
Cut 1 Preselection	Trigger, ID, leptons with opposite charge and $p_T(\mu_1) > 15$ GeV and $p_T(\mu_2) > 10$ GeV
Cut 2 Missing transverse energy \cancel{E}_T	$\cancel{E}_T > 20$ GeV
Cut 3 $Sig(\cancel{E}_T)$	$Sig(\cancel{E}_T) > 7$ (for $N_{Jet} > 0$)
Cut 4 $M_{min}^T(l, \cancel{E}_T)$	$M_{min}^T(\mu, \cancel{E}_T) > 55$ GeV
Cut 5 Invariant mass $M_{\mu\mu}$	15 GeV $< M_{\mu\mu} < 80$ GeV
Cut 6 Sum of $p_T^l + p_T^{l'} + \cancel{E}_T$	100 GeV $< p_T(\mu_1) + p_T(\mu_2) + \cancel{E}_T < 160$ GeV
Cut 7 H_T (scalar sum of p_T^{jet})	$H_T < 70$ GeV
Cut 8 Lepton opening angle $\Delta\phi_{\mu\mu}$	$\Delta\phi_{\mu\mu} < 2.0$

TABLE I: Summary of the selection criteria for a Higgs mass M_H dependent selection.

further background.

$t\bar{t}$ events are further rejected by a $H_T < 70$ GeV, the scalar sum of the p_T of good jets in the event.

Finally, the spin correlations in the decay of the Higgs boson are used. The leptons of the Higgs decay tend to have a small opening angle, whereas leptons from most of the backgrounds are expected to be back-to-back. Thus it is required that the opening angle between the leptons in the transverse plane $\Delta\phi_{\mu\mu}$ is smaller than 2.0. The angle $\Delta\phi_{\mu\mu}$ after preselection is shown in Fig. 3.

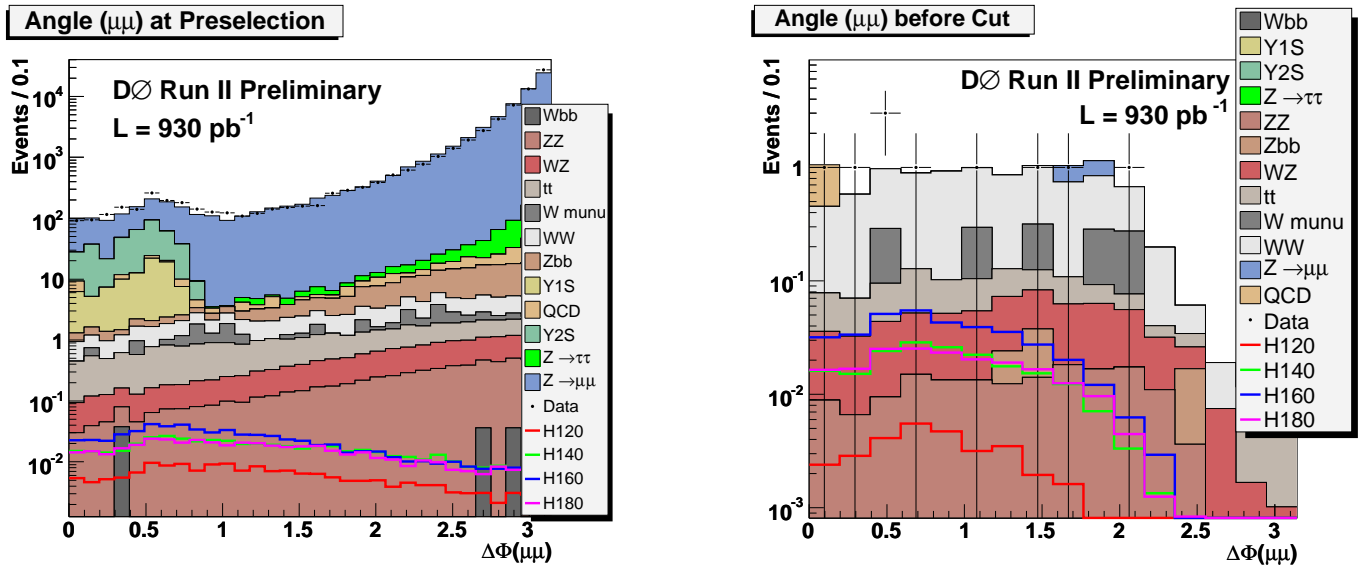


FIG. 3: Distribution of the lepton opening angle after preselection (left) and after all other cuts are applied (right). The expected signal, multiplied by a factor of 10, for the Standard Model Higgs is also shown.

III. MONTE CARLO SIMULATION OF SIGNAL AND BACKGROUND

The signal and Standard Model background processes have been generated with PYTHIA 6.319 [9] using the CTEQ6L parton distribution functions, followed by a detailed GEANT-based [10] simulation of the DØ detector. The overall detection efficiency ranges from $(3.5 \pm 0.1)\%$ to $(13.8 \pm 0.3)\%$ depending on the Higgs mass. Table II summarizes the event numbers for different Higgs masses. Using the NLO cross sections calculated with HDECAY [11] and HIGLU [12]

and branching fractions BR of 0.1057 ± 0.0022 for $W \rightarrow \mu\nu$ [13], the expected number of events for $H \rightarrow WW^* \rightarrow \mu\mu$ is $0.351 \pm 0.006(\text{stat})$ events.

The $Z/\gamma \rightarrow ll$ cross section is calculated with CTEQ6.1M PDFs as $\sigma(Z/\gamma \rightarrow ll) = \sigma_{LO} \times K_{QCD}(Q^2)$, with the LO cross section calculated by Pythia LO PDF and the K_{QCD} at NNLO with NLO PDF, calculated according to [14, 15]. The cross section times branching ratio of $Z/\gamma \rightarrow ll$ production in the invariant mass region $60 \text{ GeV} < M_{ll} < 130 \text{ GeV}$ is $\sigma \times BR = 241.6 \text{ pb}$. The $W \rightarrow \mu\nu$ background level is calculated with NNLO corrections and CTEQ6.1M as listed in [15]. For inclusive W boson production with decays into a single lepton flavor state this value is $\sigma \times BR = 2583 \text{ pb}$. The calculations of Ref. [16] are used for $t\bar{t}$ production with $\sigma \times BR = 0.076 \text{ pb}$ with single flavor lepton decays of both W bosons. The NLO WW , WZ and ZZ production cross section values are taken from Ref. [17] with $\sigma \times BR = 0.15 \text{ pb}$ for WW , $\sigma \times BR = 0.014 \text{ pb}$ for WZ and $\sigma \times BR = 0.002 \text{ pb}$ for ZZ production with decay into a single lepton flavor state. The background due to multijet production is determined from the data using a sample of di-muon events with inverted muon quality cuts.

The normalization used in this analysis is a factor that scales the NNLO $Z/\gamma^* \rightarrow \mu\mu$ cross section (see Fig. 1) to the data in the mass region $60 \text{ GeV} < M_{\mu\mu} < 120 \text{ GeV}$. The estimated data sample size was found to be of the order of $\sim 930 \text{ pb}^{-1}$. Data/MC muon correction factors have been applied to MC before normalization to $Z/\gamma^* \rightarrow \mu\mu$. No data/MC muon correction factors for trigger efficiencies have been applied and they are absorbed in the normalization to $Z/\gamma^* \rightarrow \mu\mu$. By using this method to estimate data sample size, the limit on the $H \rightarrow WW^* \rightarrow \mu\mu$ cross section is calculated relative to the NNLO $Z/\gamma^* \rightarrow \mu\mu$ cross section. Systematic uncertainties, coming from the luminosity determination and from data/MC correction factors are canceled by using this normalization procedure.

A summary of the background contributions together with events observed in the data after the final selection is shown in Table III.

Various sources of systematic uncertainties affect the background estimation and the signal efficiency of $H \rightarrow WW^*$ production: theoretical uncertainty of WW , $t\bar{t}$ and Z/γ^* production cross sections, Jet Energy Scale (JES), muon reconstruction efficiencies and resolutions. Since the WW production is the dominant background for Higgs bosons, the uncertainty on the WW production cross section is a major contribution (5%). The uncertainty in the QCD background determination contributes with 4%. The Jet Energy Scale contributes with 1% and the momentum resolution with 11%. Until the systematic uncertainties are completely studied, conservative systematic errors of 10% and 16% for the signal and background respectively are used. The systematic uncertainty on the normalization factor is conservatively taken to be 5%. It results from the NNLO $Z/\gamma^* \rightarrow ll$ cross section uncertainty (4%), PDF uncertainty (2%) and the statistical error on data/MC normalization factor (1%).

IV. SUMMARY

A search for the Higgs boson is presented in $H \rightarrow WW^* \rightarrow \mu\mu$ decays in $p\bar{p}$ collisions at a center-of-mass energy of $\sqrt{s} = 1.96 \text{ TeV}$. The data, collected from April 2002 to November 2005 with the Run II DØ detector, correspond to an integrated luminosity of the order of $\sim 930 \text{ pb}^{-1}$. The number of events observed is consistent with expectations from standard model backgrounds.

-
- [1] T. Han, A. Turcot, R.-J. Zhang, Phys. Rev. D. 59, 093001 (1999).
 - [2] M. Carena *et al.* [Higgs Working Group Collaboration], “Report of the Tevatron Higgs working group”, hep-ph/0010338.
 - [3] K. Jakobs, W. Walkowiak, ATLAS Physics Note, ATL-PHYS-2000-019.
 - [4] J. Elmsheuser, M. Hohlfeld, DØ Note 4759; Phys. Rev. Lett. 96, 011801 (2006)
 - [5] M. Titov, DØ Note 5063-CONF.
 - [6] DØ Collaboration, V. Abazov *et al.*, to be published in Nucl. Instrum. Methods A; arXiv:physics/0507191.
 - [7] DØ Collaboration, S. Abachi *et al.*, Nucl. Instrum. Methods Phys. Res. A **338**, 185 (1994).
 - [8] V. Abramov *et al.*, Nucl. Instrum. Meth. A **419**, 660 (1998).
 - [9] T. Sjöstrand *et al.*, Comp. Phys. Comm. **135**, 238 (2001).
 - [10] R. Brun and F. Carminati, CERN Program Library Long Writeup W5013, 1993 (unpublished).
 - [11] A. Djouadi *et al.*, Comput. Phys. Commun. **108**, 56 (1998).
 - [12] M. Spira, Report DESY T-95-05 (October 1995), arXiv:hep-ph/9510347.
 - [13] Particle Data Group, S. Eidelman *et al.*, Phys. Lett. B **592**, 1 (2004).
 - [14] R. Hamberg, W.L. van Neerven, and T. Matsuura, Nucl. Phys. **B359**, 343 (1991) [Erratum-ibid. **B644**, 403 (2002)].
 - [15] T. Nunnemann, DØ Note 4476.
 - [16] N. Kidonakis and R. Vogt, Phys. Rev. D **68**, 114014 (2003).
 - [17] J. M. Campbell and R. K. Ellis, Phys. Rev. D **60**, 113006 (1999).
 - [18] T. Junk, Nucl. Instr. and Meth., A434(1999) 435.

- [19] E. Arik, O. Cakir, S.A Cetin and S. Sultansoy, arXiv:hep-ph/0502050.
- [20] E. Arik, M. Arik, S. A. Cetin, T. Conka, A. Mailov and S. Sultansoy, Eur. Phys. J. C **26**, 9 (2002).

$H120$	$H140$	$H160$	$H180$	$H200$
0.030 ± 0.001	0.186 ± 0.003	0.351 ± 0.006	0.187 ± 0.003	0.075 ± 0.001

TABLE II: Event numbers with statistical errors for $H \rightarrow WW^* \rightarrow \mu\mu$ for four different Higgs masses between 120 and 180 GeV.

TABLE III: Number of signal and background events expected and number of events observed after all selections are applied. Only statistical uncertainties are given.

QCD	tt	Wbb	$W + jet/\gamma$	WW	WZ	Υ
0.6 ± 0.6	0.48 ± 0.05	0 ± 0	0.97 ± 0.43	6.6 ± 0.1	0.40 ± 0.01	0 ± 0

Zbb	ZZ	$Z \rightarrow \mu\mu$	$Z \rightarrow \tau\tau$	Sum	$Data$
0.04 ± 0.02	0.13 ± 0.01	0.6 ± 0.4	0 ± 0	9.8 ± 0.8	9 ± 3.0